



Article

Fabrication of Superhydrophobic Wood Surface by Etching Polydopamine Coating with Sodium Hydroxide

Zede Yi , Bo Zhao, Murong Liao and Zhiyong Qin * 

School of Resources, Environment and Materials, Guangxi University, Nanning 530000, China; mk172yzd@163.com (Z.Y.); zhao2141716947@163.com (B.Z.); mr_liaomr@163.com (M.L.)

* Correspondence: qinzhiyong@gxu.edu.cn; Tel.: +86-771-323-6100

Received: 2 August 2020; Accepted: 26 August 2020; Published: 31 August 2020



Abstract: Superhydrophobic treatment of wood surfaces can effectively prevent the contact between the external moisture and wood, which improves the service life of the wood. In this study, different rough surfaces of wood were constructed, derived from the self-polymerization of dopamine (DA) in weak base solution to form a polydopamine (PDA) coating and the deprotonation of the PDA coating in a strong base solution. Furthermore, octadecyltrichlorosilane (OTS) was used as a low-surface-free-energy agent to modify rough surface in order to prepare superhydrophobic woods: Wood@PDA–NaOH–OTS and the Wood@PDA–NaOH/SiO₂–OTS. The contact angles (CAs) and sliding angles (SAs) of the resulting superhydrophobic woods were tested. The results showed that the CA and SA of the Wood@PDA–NaOH–OTS were 151° and 4.8°, respectively; the CA and SA of the Wood@PDA–NaOH/SiO₂–OTS were 155.1° and 5.0°, respectively. Surface electron microscopy (SEM) images presented that NaOH successfully etched the PDA coating, and the roughness was further improved by adding nano-SiO₂. Atomic force microscope images (AFM) revealed that the nano-SiO₂ particles could effectively provide nanolevel roughness, which was beneficial to the wood's superhydrophobic properties. In addition, the obtained superhydrophobic wood possessed strong surface stability and anti-loss property, as well as resistance to acid-base solution and organic solvent.

Keywords: polydopamine; alkaline etch; superhydrophobic wood; stability

1. Introduction

As a natural renewable and environmentally friendly material, wood occupies an important position in fields of wooden structure architectural design, interior/exterior decoration and furniture manufacturing due to its superior resources and mechanical properties [1]. Wood's peculiar matrix (cellulose and hemicellulose) and structure endow it with excellent mechanical and hygroscopic properties. Cellulose and hemicellulose contain large numbers of hydrophilic groups (e.g., hydroxyl or hydroxymethyl) that easily form hydrogen bonds and adsorb external water molecules. As wood is a porous material it can uptake water. However, the hygroscopic properties of wood may cause wood and its products to tend to crack and deform in use and storage. This will not only influence use value and performance, but also aggravate mildew, decaying and degradation, endangering service safety and life of wooden products [2]. The strategy of superhydrophobic modification of wood is proposed to overcome the above challenges. Superhydrophobic modification endows wood with unique wettability and improves the functional properties of wood such as anti-corrosion, waterproof, dimension stability, etc., which can make wood better meet the needs of multifunctional using [3–6].

Superhydrophobic phenomenon, such as lotus effect, is common in nature and favored by materials scientists. Studies have found that superhydrophobic phenomenon is attribute to the interaction

of micro-nano secondary structures and low surface energy materials [7–9]. Inspired by the lotus effect, a bionics strategy is proposed to prepare superhydrophobic material: constructing a micro-nano rough structure on the material surface and modifying the micro-nano substrate with low function. Methods applicable to bionic construction of wood superhydrophobic surface mainly include surface coating method, sol–gel method, hydrothermal method, layer by layer self-assembly method, wet chemical method and chemical vapor deposition method commonly used in low surface energy modification, etc. [10–13]. Yang et al. designed a new strategy to prepare superhydrophobic wood that the nano-SiO₂–PDMS coating were deposited onto the wood surface and OTS was grafted on the SiO₂ microsphere surface, and its CA and SA were 151° and 6°, separately [14]. In Che et al. the alkyl SiO₂ nanoparticles were deposited and assembled to the surface of the polytetrafluoroethylene (PTFE) hollow fiber membrane, and the low surface energy modification of alkyl SiO₂ nanoparticles was further applied by perfluorodecyl triethoxysilane to construct superhydrophobic structure on the membrane surface [15]. Ntelia developed a new strategy that superhydrophobic Paraloid B72 coatings were produced by embedding silica nanoparticles into the acrylic polymer, and hydrophobicity was enhanced with the nanoparticle concentration leading ultimately to superhydrophobicity [16]. Bohinc et al. stated that the increased adhesion of bacteria on more rough surfaces was the interplay between the increasing effective surface and increasing number of defects on the surface [17]. Yue et al. revealed hydrophobic SiO₂ nanoparticles were formed by the ammonia-hexamethyldisilazane (HMDS) vapor treatment and a superhydrophobic coating was in situ fabricated on a wood surface [18]. Ghazali realized two layers system of super-amphiphobic coating by using functionalized nano-Al₂O₃ incorporated in polyvinylidene fluoride (PVDF) [19]. The so-called superhydrophobic surface refers to the surface where the contact angle (CA) of water is greater than 150° and the sliding angle (SA) is less than 10°. The traditional strategy of preparing superhydrophobic surface is that inorganic nanoparticles are introduced to provide roughness, but the interfacial bonding performance between inorganic nanoparticles and substrate surface was neglected. The superhydrophobic surface lacks stability and durability, therefore it is urgent to search for a polymer with excellent adsorption to improve the interfacial bonding performance between inorganic nanoparticles and substrate.

The adhesive proteins secreted by marine mussels through byssus are characterized by high strength, high toughness, water resistance and strong adhesion, which can make them adhere to almost all the substrate materials [20,21]. Inspired by the protein structure secreted by mussels, researchers have found that catechol has similar structure and properties to the protein secreted by mussels [22,23]. In addition, the catechol structure in the PDA has antibacterial properties [24]. Dopamine (DA) contains catechol structure and amino groups, which can form polydopamine (PDA) coating owing to the self-polymerization in mild reaction conditions. The PDA coating can form hydrogen bond association, electrostatic attraction, chelating and covalent bond interaction with other matrix materials and possesses a great potential in secondary functionalization [25,26]. PDA modification has become one of the most attractive modification methods in the field of surface-modification engineering due to its wide applicability, effective modification process and multifunctional properties [27–29]. A research indicated that the PDA coating formed by solution polymerization was difficult to dissolve in strong acid and strong polar organic solvents [26]. According to the formation mechanism of the PDA proposed in the existing literature, the joint action of covalent bond and non-covalent bond is one of the most comprehensive explanations. However, PDA is prone to deprotonation (H⁺) in alkaline environment, which results in covalent bond destruction, collapse and decomposition of the PDA, and the surface structure of the PDA coating is changed [30–32].

Because PDA has strong adhesion performance, it is possible to solve the problem of weak binding ability between inorganic nanoparticles and substrate, and a stable superhydrophobic surface of wood is constructed. To date, there are few reports on the biomimetic construction of wood superhydrophobicity by PDA coating. Thus, due to the deprotonation characteristic of the PDA, an alkali etching method was proposed to construct the roughness structure of wood surface in the study. Based the lotus effect, inorganic nano-SiO₂ particles were further introduced into the structure to

improve the wood surface roughness. The adhesion between inorganic nanoparticles and the substrate surface may be improved because of the existing of the remaining PDA coating. In the last step, fluorine-free octadecyltrichlorosilane (OTS) was used to construct low functionalized surface to prepare superhydrophobic wood [33]. The surface wettability of superhydrophobic wood was investigated with different etching time, the samples surface structure was represented by surface electron microscopy (SEM) and atomic force microscope (AFM), and the surface resistance and chemical stability were tested.

2. Experimental Section

2.1. Materials

Pinus sylvestris var. mongolica, 12 years old with an average growth-ring width of 2.5 mm, was purchased from Shanghai Jimuwu Co., Ltd. (Shanghai, China). Wood blocks of 20 mm (longitudinal) × 10 mm (tangential) × 5 mm (radial) were washed twice with deionized water and anhydrous ethanol, respectively. After being oven-dried at 60 °C for 72 h, the moisture contents of wood samples were regulated under ambient condition for 24 h.

DA hydrochloride, tris(hydroxymethyl)aminomethane (Tris) and OTS were purchased from Aladdin Chemistry Co., Ltd. (Shanghai, China). Anhydrous ethanol, sodium hydroxide (NaOH), hydrochloric acid (HCl), acetone, n-hexane and tetrahydrofuran were purchased from Tianjin Fuyu Fine Chemical Co., Ltd. (Tianjin, China). Hydrophilic nano-SiO₂ (purity ≥99.8%) with a particle size of 15 ± 5 nm was acquired from Shanghai Keyan Industrial Co., Ltd. (Shanghai, China). Deionized water was self-made in the laboratory. All chemical reagents were used as received without further purification.

2.2. Methods

2.2.1. Wood Modified by PDA

Previous studies have shown that the PDA coating is thickest after 24 h of deposition [31,34]. Therefore, the DA polymerization time was set at 24 h in this study. The pH value of the DA solution (0.2%, *m/v*) was adjusted to 8.5 ± 0.1 by using the alkaline buffer Tris solvent. The wood samples were placed together with the DA solution in a reaction kettle at a constant temperature of 60 °C for 24 h, allowing the DA to form a dense PDA coating on the wood surface. After the reaction, the resulting surface was washed with deionized water for three times and oven-dried at 60 °C for 24 h. The samples were labeled as Wood@PDA.

2.2.2. Etching of the Wood@PDA with NaOH

To study the effect of NaOH etching time on Wood@PDA surface, different etching time was employed. The Wood@PDA samples were first immersed in NaOH solution (2%, *w/w*). Subsequently, the samples were taken out after magnetic stirring for 5 min, 30 min, 1 h, 2 h and 5 h, respectively and then dried at 60 °C for 8 h. Ultimately, the etched surfaces were further washed with deionized water to remove the excess NaOH and the PDA particles falling off in the process of etching and dried at 60 °C for 24 h.

2.2.3. Etching of the Wood@PDA with NaOH/SiO₂

To obtain a rougher surface, nano-SiO₂ particles were introduced in the process of NaOH etching. Two hundred grams NaOH/SiO₂ aqueous solution (composed of 2 g NaOH, 1 g nano-SiO₂ and 197 g deionized water) was prepared, and the Wood@PDA samples were first immersed in the solution. Subsequently, the samples were taken out after magnetic stirring for 5 min, 30 min, 1 h, 2 h and 5 h, respectively and dried at 60 °C for 8 h. Ultimately, the etched surfaces were further washed with deionized water to remove the excess NaOH and the PDA particles falling off in the process of etching and dried at 60 °C for 24 h.

The modification conditions of the above methods are shown in Table 1.

Table 1. Modified conditions.

Pretest Sample	Treatment Time	Temperature	Solution	Oven-Dried Time and (Temperature)	Posttest Sample
Wood	24 h	60 °C	DA	24 h (60 °C)	Wood@PDA
Wood@PDA	5 min–5 h	Room Temperature	NaOH	24 h (60 °C)	Wood@PDA–NaOH
Wood@PDA	5 min–5 h	Room Temperature	NaOH/SiO ₂	24 h (60 °C)	Wood@PDA–NaOH/SiO ₂

2.2.4. Low Surface Energy Treatment

A 2 wt.% OTS solution was prepared with n-hexane. The samples which were etched by NaOH or NaOH/SiO₂ were added into OTS solution and stirred by magnetic force for 2 h. The surfaces of the samples were treated with low surface energy by grafting long-chain silane. After the reaction, the unreacted OTS was removed by washing with n-hexane twice. Then the samples were dried for 24 h at room temperature to obtain superhydrophobic wood. For the convenience of difference, the superhydrophobic wood prepared by above methods were, respectively recorded as Wood@PDA–NaOH–OTS and the Wood@PDA–NaOH/SiO₂–OTS.

2.3. Testing and Characterization

2.3.1. Surface Wettability of Superhydrophobic Wood

The CA and SA measurements were performed with a CA meter (KRÜSS DSA100E, Hamburg, Germany). The CAs of samples surface were measured by sessile drop method, and the droplet size was 5 µL. The droplet staying on the solid surface was a dynamic process because of its obvious wetting behavior on the non-superhydrophobic surface [35]. However, the samples prepared in this experiment were superhydrophobic surface (or nearly superhydrophobic surface), and the droplet formed a stable water droplet state on the wood surface. Cassie and Baxter believed that there was a phenomenon of composite contact on the solid surface, i.e., the droplets would not infiltrate into the grooves on the solid surface and there was trapped air under the droplet, which was called Cassie–Baxter model. Therefore, droplet spreading and permeation cannot occur on a superhydrophobic surface. In this experiment, the static CA was the instantaneous CA of water droplets on the wood surface for 5 s. SAs were determined by the minimum tilt angle of the sample platform at which a water droplet (5 µL) rolled off the surface. Three random points of the same sample were tested and averaged.

2.3.2. CIELab Color of Samples with Different Etching Time

In order to quantify the color of samples with different etching time, an automatic chromometer (ADCI-60-C, Beijing Chentaike Instrument Technology Co., Ltd., Beijing, China) was used. The chromaticity parameters of samples at the center and two diagonal points were measured with a measuring probe. The surface of the same sample was measured three times, and the average value was taken.

2.3.3. Analysis of Surface Microstructure

The tangential section of four wood samples was characterized by SEM (Hitachi SU8220, Tokyo, Japan). After sprayed with gold, the samples surface was observed with SEM. The magnification was 2000 and 40,000 times, and the voltage and the resolution of analysis mode were 5.0 kV and 3.0 nm, respectively.

An AFM (Agilent 5500, Palo Alto, Santa Clara, CA, USA) was used to observe the tangential section of the two superhydrophobic wood samples. The observation range was 0–100 µm, and automatic scaling and focusing were used. The 3D maps of the samples surface were collected in the tapping mode.

2.3.4. Analysis of the Surface Resistance of Superhydrophobic Wood

The samples were treated by ultrasonic vibration to study the influence of different vibration time on the stability of the PDA coating. The specific implementation method was that the superhydrophobic wood samples were put into the water and vibrated for 8 h in the ultrasonic vibration instrument (KQ2200, Kunshan Ultrasonic Instrument Co., Ltd., Kunshan, China) with power of 100 W and frequency of 42 KHz. Three wood samples were randomly taken out every 1 h as a group, and the CAs and SAs of their surfaces were measured and averaged in each group. In addition, considering that wooden products are usually used outdoors, a simulated rain experiment was set up, as shown in Figure 1. Three samples of the Wood@PDA–NaOH–OTS and the Wood@PDA–NaOH/SiO₂–OTS were, respectively pasted on the surface of glass plate with an inclination angle of 30°. The sample surface was 20 mm away from the water outlet, the water flow speed was 2 L/h, and the outlet diameter was 2 mm. The CAs and SAs of the flow area after treatment of 3, 6, 9, 12 and 24 h were respectively measured and the average values were taken.

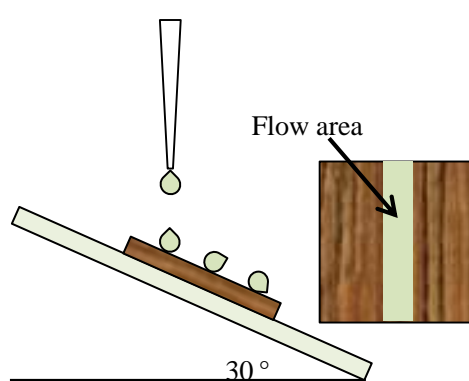


Figure 1. Schematic diagram of water resistance test for superhydrophobic wood.

2.3.5. Chemical Stability of Superhydrophobic Wood Surface

To evaluate the acid-base stability of superhydrophobic wood, the samples were respectively soaked in HCl and NaOH aqueous solutions with pH values of 1, 3, 5, 7, 9 and 12. Moreover, 100 mL of n-hexane, absolute ethanol, acetone and tetrahydrofuran were separately used to soak the wood samples to evaluate the organic solvents resistance of samples surface. Three samples were placed in each group and soaked for 24 h, then the samples were taken out and dried. The CAs and SAs of the samples surface were, respectively measured and the average values were taken in each group.

3. Results and Discussion

3.1. Analysis of Surface Wettability

The PDA could form negatively charged DA quinone with deprotonation treatment, then a chemical bond formed between it and the function group of the wood surface by the REDOX reaction [36]. Figure 2 shows that the positive and negative charges on the surface of the Wood@PDA samples were uniformly distributed and showed electrical neutrality. However, PDA lost protons (H⁺) on the surface of the Wood@PDA–NaOH samples, showing negative electroactivity and electrostatic attraction, which made the PDA coating relatively stable. There were a large number of hydrogen bonds and electrostatic attraction on the surface of the Wood@PDA–NaOH/SiO₂, thus its surface had better stability.

After low surface energy treatment, the results of surface wettability of the etched samples are shown in Figure 3. It could be seen that the CAs of wood samples had up to 150° and the SAs were all below 10°. The CA and SA of the Wood@PDA–NaOH–OTS were 151° and 4.8°, respectively. However, the Wood@PDA–NaOH/SiO₂–OTS had a larger CA reaching a maximum of 155.1° and a SA of 5.0°.

It should be noticed that there was little change of CA in different etching time. The reason was that the PDA was shed deeply with increasing etching time, but it was collapsed layer-by-layer. Therefore, the surface roughness of the etched samples displayed little change and the effect of etching time on roughness was not obvious.

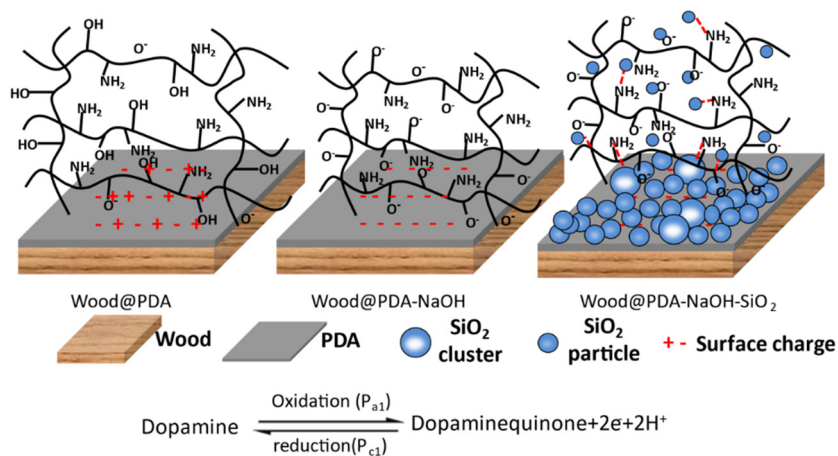


Figure 2. Model diagram of polydopamine (PDA) deprotonation process.

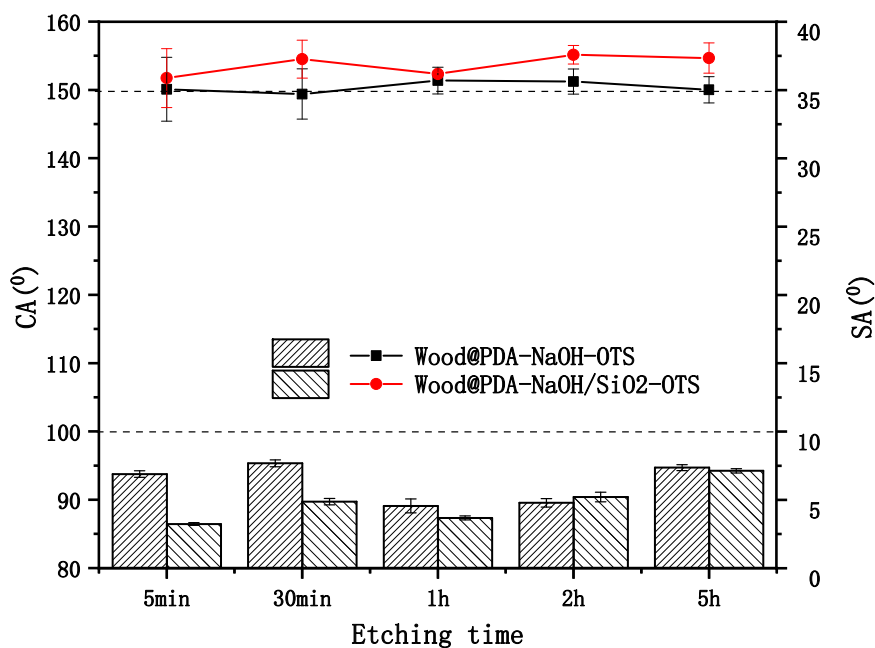


Figure 3. Contact angles (CAs) (in lines) and sliding angles (SAs) (in bars) of the Wood@PDA–NaOH–OTS and the Wood@PDA–NaOH/SiO₂–OTS.

3.2. Colorimetric Analysis of Wood Sample Surface

To make the surface rougher, the Wood@PDA were immersed in a NaOH solution. The images of color change with different time treatments are presented in Figure 4. As shown, the color of the etched samples gradually lightened with the increase of etching time. The reason was that the PDA could be flaked by strong alkaline. When soak time was extended further, more PDA was shed. After five hours of treating, the surface color of the etched samples become lightest, indicating that the PDA coating was successfully etched in the strong alkaline solution. This was consistent with the chromaticity parameters in Table 2. *L**, *a** and *b** had an rising trend with the increase of etching time as a whole, which indicated that the surface of the samples tended to be brighter, redder and yellower.

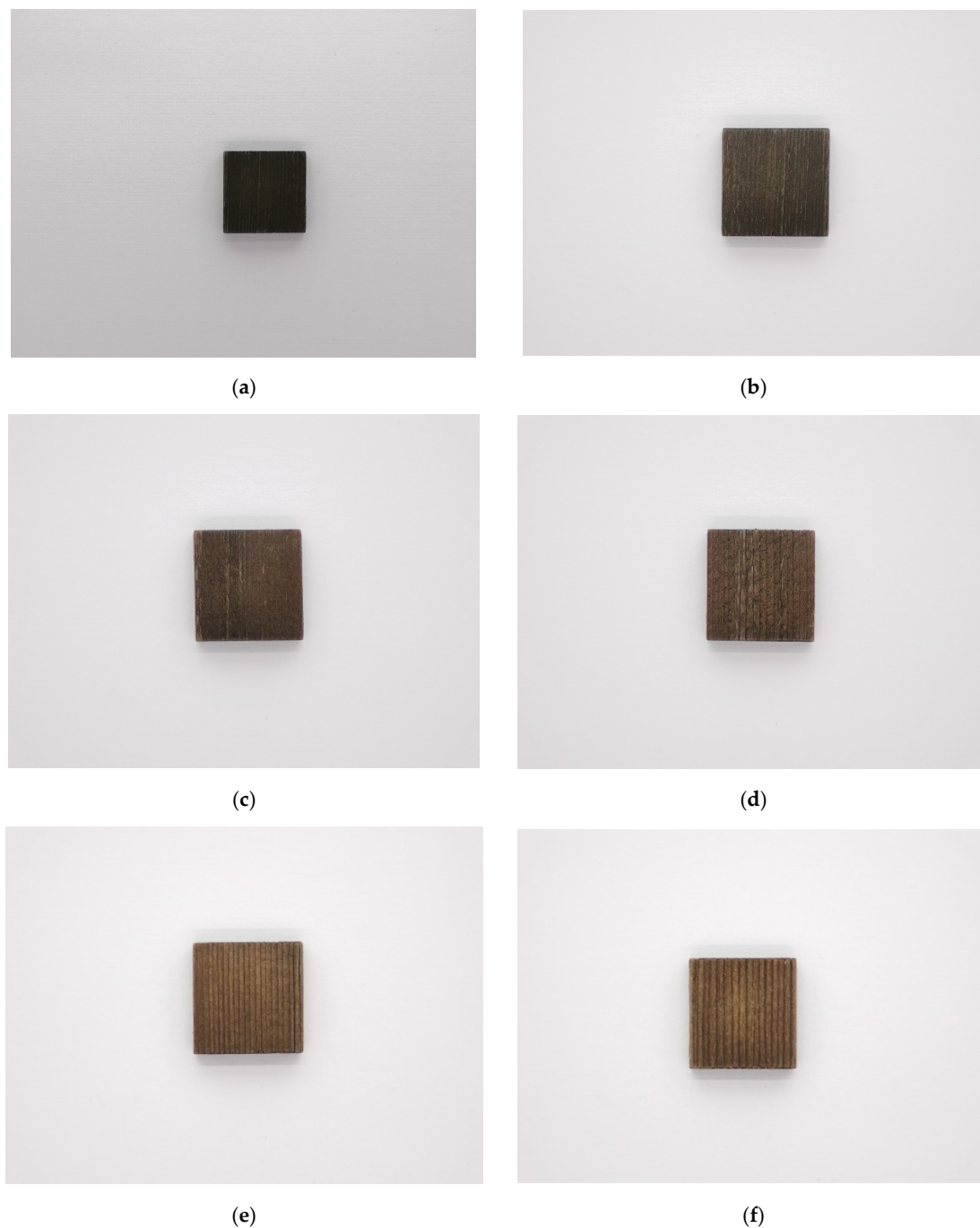


Figure 4. Images of the etched samples with different etching times: (a) Control; (b) etching for 5 min; (c) etching for 30 min; (d) etching for 1 h; (e) etching for 2 h; (f) etching for 5 h.

Table 2. Chromaticity parameters of the etched samples with different etching times.

Etching Time	L^*	a^*	b^*	ΔE^*
0 min	21.40 (1.29)	11.20 (3.07)	4.23 (1.32)	74.32 (1.69)
5 min	22.91 (0.63)	11.03 (5.96)	6.51 (1.48)	73.02 (1.68)
30 min	24.40 (0.60)	20.12 (1.31)	5.42 (0.76)	73.39 (0.96)
1 h	26.61 (0.68)	18.29 (1.97)	7.99 (0.40)	70.86 (1.12)
2 h	28.65 (0.30)	11.89 (2.12)	14.47 (0.19)	68.32 (0.54)
5 h	32.58 (0.78)	30.29 (7.61)	17.21 (3.91)	68.27 (5.61)

L^* —brightness index; a^* —chromaticity index of metric red green axis; b^* —chromaticity index metric yellow blue axis; ΔE^* —total chromatic aberration. Data in brackets are standard deviation.

3.3. Surface Microstructure of Superhydrophobic Wood

The microstructure of original wood and modified wood sample with SEM are shown in Figure 5. Figure 5a was the cell wall surface of the original wood, showing a smooth morphology. In Figure 5b, the surface of the Wood@PDA was also relatively smooth, which was consistent with the research of Wang [34]. This indicated that the PDA coating without etching did not have hydrophobic properties. The surface of the Wood@PDA–NaOH–OTS showed many cracks and protruding rough in Figure 5c, owing to etching in NaOH. From the further enlarged Figure 5c, it could be seen that the protruding microstructure was still rough, indicating that it had the condition of superhydrophobic primary micro-nano structure roughness. The rough surface conducted by alkaline etching was confirmed. In Figure 5d, the Wood@PDA–NaOH/SiO₂–OTS displayed many cracks and protruding rough too, and there were plenty of particles on the surface. Those nanoparticles may be the inorganic nano-SiO₂. In addition, as nano-SiO₂ agglomerates, it can be seen in the enlarged Figure 5d that SiO₂ clusters were loaded on the surface of the PDA coating, forming a more obvious micro-nano rough structure. The introduction of the nano-SiO₂ improved the nanoscale roughness of wood surface.

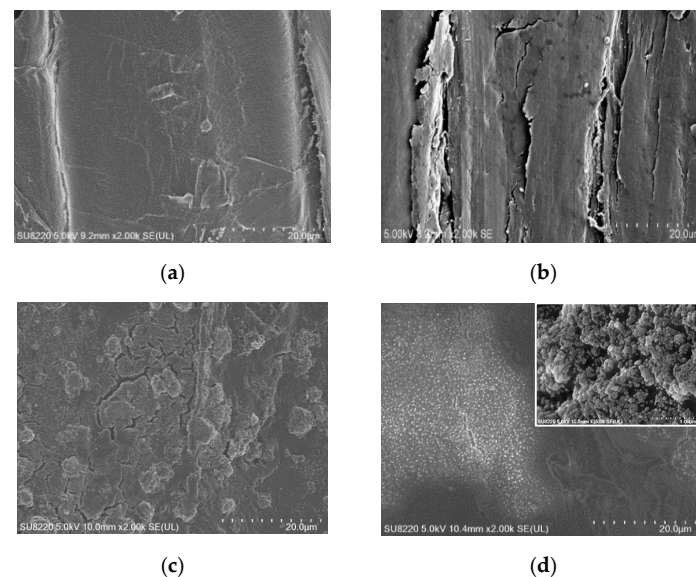


Figure 5. SEM images of wood samples. (a) Original wood (2×10^3); (b) Wood@PDA (2×10^3); (c) Wood@PDA–NaOH–OTS (2×10^3 , 40×10^3); (d) Wood@PDA–NaOH/SiO₂–OTS (2×10^3 , 40×10^3).

The 3D structure of superhydrophobic wood with AFM is shown in Figure 6. On the surface of the Wood@PDA–NaOH–OTS, the ravine-like etching could be significantly observed, and the surface protrusion height was about 30.7 nm. For Wood@PDA–NaOH/SiO₂–OTS, the surface became relatively smooth due to the increase of protruding roughness, and the surface protrusion height of it was about 4.5 nm. However, the specific surface area increased, so the Wood@PDA–NaOH/SiO₂–OTS had better superhydrophobic property.

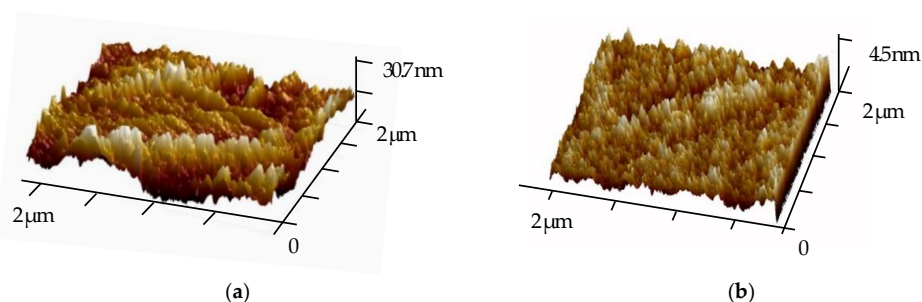


Figure 6. AFM images. (a) Wood@PDA–NaOH–OTS; (b) Wood@PDA–NaOH/SiO₂–OTS.

According to Cassie–Baxter model, it can be considered that the apparent contact surface consists of the solid–liquid contact area and the liquid–gas contact area. When the droplet is in equilibrium, the following Equation (1) can be obtained:

$$\cos \theta^* = f_s(1 + \cos \theta_e) - 1 \quad (1)$$

where f_s is the area fraction occupied by liquid–solid in the composite contact surface, which is less than 1. θ^* is the apparent CA, and θ_e is the intrinsic CA of the solid–liquid contact surface. In the hydrophobic region, the smaller the value is, the greater the apparent CA is [37]. In this study, as surface roughness increased, the actual contact area of liquid–gas was larger than that of liquid–solid, i.e., the f_s value of the Wood@PDA–NaOH/SiO₂–OTS was smaller. Thus, the material exhibited superior superhydrophobic properties. The finding was consistent with Lou [38], indicating that the primary condition for biomimetic fabrication of wood superhydrophobic surface is to construct rough micro–nano structure. Superhydrophobic wood can isolate the contact with external water to a certain extent, which is very important to improve the service life of wood.

3.4. Anti-Loss Analysis

The anti-loss properties of samples was studied using continuous flow scouring and ultrasonic vibration; the results are shown in Figure 7. In Figure 7a, Wood@PDA–NaOH–OTS showed excellent stability and maintained superhydrophobic ability under sustained flow scouring. The micro–nano rough structure of superhydrophobic surface was still maintained. It should be noted that the superhydrophobic performance was slightly lost after 12 h, but it was close to the superhydrophobic level. As for the Wood@PDA–NaOH/SiO₂–OTS, the CA was still over 150° after being scoured by flow for 24 h. The roughness provided by PDA overcame the problem of weak interface bonding between inorganic nanoparticles and organic matrix, resulting in showing stronger anti-loss ability. The SAs of superhydrophobic samples were always less than 10° under 24 h treatment, and there was not much difference between them. From Figure 7b, the CAs of all modified samples appeared the decline of different degree after the continuous ultrasonic vibration. Wood@PDA–NaOH–OTS rapidly lost its superhydrophobic properties after one hour. The SA was greater than 10° after the five-hour treatment. However, the Wood@PDA–NaOH/SiO₂–OTS did not lose its superhydrophobic properties until six hours later, and it was still close to the superhydrophobic level. The SAs were always less than 10° under the eight-hour treatment. As a result of the PDA deprotonation under alkaline conditions, part of the Wood@PDA–NaOH–OTS covalent bond was destroyed, resulting in that the remaining PDA on the wood surface became looser and shed in the continuous ultrasonic vibration, thus superhydrophobic performance decreased. Considering that DA contains a large number of catechol and pyrogallol groups which can interact with wood and nano-SiO₂ by hydrogen bond and hydrophobic, inorganic nano-SiO₂ was introduced in the process of alkali etching on the PDA surface, resulting in that the nano-SiO₂ formed a strong adhesion with wood surface and further improved the stability of superhydrophobic performance.

3.5. Surface Chemical Stability

The chemical stability of superhydrophobic surface was investigated by soaking superhydrophobic wood samples in different pH solutions and organic solvents. As shown in Figure 8, the SAs of superhydrophobic wood were always below 10°. It can be seen from Figure 8a that the CAs of the Wood@PDA–NaOH–OTS and the Wood@PDA–NaOH/SiO₂–OTS did not change obviously in a wide pH range. However, when the pH value was greater than 9, the superhydrophobic performance continued to decline, which may be caused by the slight shedding of nanoparticles. In Figure 8b, the CAs of samples maintained above 150°, indicating that Wood@PDA–NaOH–OTS and the Wood@PDA–NaOH/SiO₂–OTS had excellent stability in organic solvents. The PDA coating could effectively improve the chemical stability of wood. After deprotonation, part of the PDA was

shed, and the residual polymer was not sensitive to the change of pH. Moreover, the PDA coating was extremely easy to obtain, and the preparation condition was mild. It can form a layer of the PDA coating on almost any substrate surface with strong adhesion.

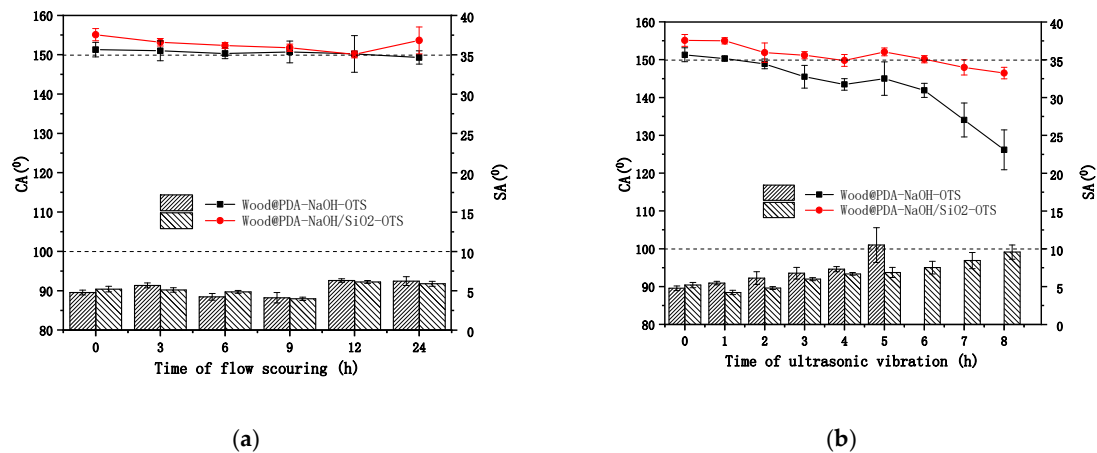


Figure 7. CAs (in lines) and SAs (in bars) of superhydrophobic wood under (a) flow scouring and (b) ultrasonic vibration.

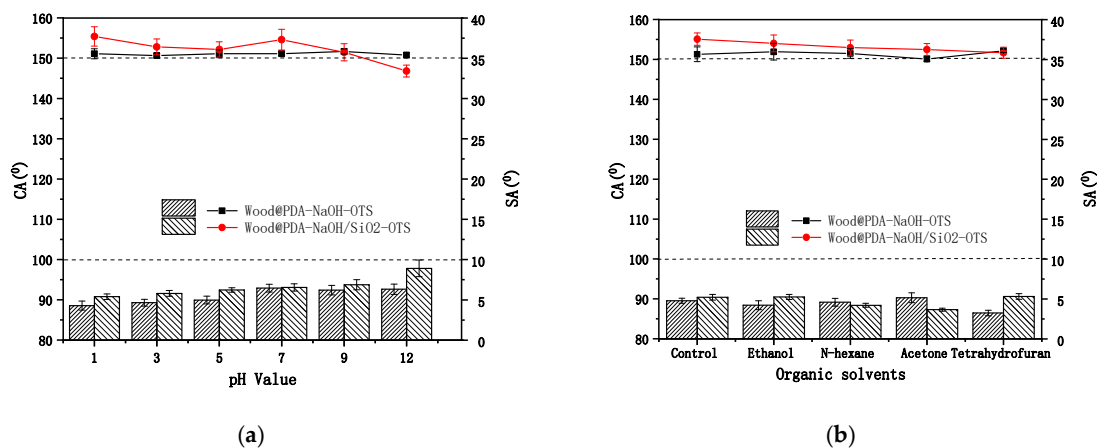


Figure 8. CAs (in lines) and SAs (in bars) of superhydrophobic wood soaked in (a) different pH solutions and (b) organic solvents for 24 h.

4. Conclusions

In this study, superhydrophobic wood surface was successfully fabricated by an alkaline etch method. It is vital that OTS was used to graft long-chain silane to achieve superhydrophobicity of wood. The effect of etching time on superhydrophobic properties of wood was not obvious. SEM and AFM images showed that the PDA coating was successfully etched by NaOH, and the roughness was further improved by adding SiO₂ nanoparticles. Wood@PDA-NaOH-OTS and the Wood@PDA-NaOH/SiO₂-OTS both exhibited excellent stability under continuous flow scouring for 24 h. The PDA coating overcame the problem of weak binding between inorganic nanoparticles and substrate. The Wood@PDA-NaOH/SiO₂-OTS group showed excellent surface stability in ultrasonic vibration, while the Wood@PDA-NaOH-OTS group had poor stability due to the tendency of the PDA particles shedding. Etched by alkali, the parts of the Wood-NaOH/SiO₂-OTS and the Wood-NaOH-OTS that were easy to peel off were removed, and the retained PDA coating had strong resistance in acid-base solution and strong organic solvents.

Author Contributions: Conceptualization, M.L. and Z.Q.; methodology, Z.Y. and M.L.; validation, Z.Y. and M.L.; investigation, B.Z. and Z.Q.; writing—original draft preparation, Z.Y. and M.L.; writing—review and editing, Z.Y., B.Z., and Z.Q. All authors have read and agreed to the published version of the manuscript.

Funding: This research was funded by the Innovation-Driven Project Funds of Guangxi (AA17204087-15) and the Fundamental Research Funds for the National Natural Science Foundation of China (Project 31790188).

Acknowledgments: The authors would like to acknowledge Guangxi University.

Conflicts of Interest: The authors declare that they have no conflict of interest.

References

1. Gu, L.B. Current status and application prospects of wood modification. *China Wood Ind.* **2012**, *26*, 3.
2. Huang, Y.H.; Feng, Q.M.; Ye, C.Y.; Sandeep, S.N.; Yan, N. Incorporation of ligno-cellulose nanofibrils and bark extractives in water-based coatings for improved wood protection. *Prog. Org. Coat.* **2020**, *138*, 105210. [[CrossRef](#)]
3. Liu, M.; Wu, Y.Q.; Yan, Q.; Tian, C.H.; Luo, S.; Li, X.G. Progress in the research of functional modification on bionic fabrication of superhydrophobic wood. *J. Funct. Mater.* **2015**, *46*, 14012–14018.
4. Liu, F.; Wang, C.Y. Research progress and preparation methods of biomimetic functional superhydrophobic wood surfaces. *Sci. Technol. Rev.* **2016**, *34*, 120–126.
5. Jia, S.S.; Liu, M.; Wu, Y.Q.; Luo, S.; Qing, Y.; Chen, H.B. Facile and scalable preparation of highly wear-resistance superhydrophobic surface on wood substrates using silica nanoparticles modified by VTES. *Appl. Surf. Sci.* **2016**, *386*, 115–124. [[CrossRef](#)]
6. Wang, K.L.; Dong, Y.M.; Yan, Y.T.; Zhang, W.; Qi, C.S.; Han, C.R.; Li, J.Z.; Zhang, S.F. Highly hydrophobic and self-cleaning bulk wood prepared by grafting long-chain alkyl onto wood cell walls. *Wood Sci. Technol.* **2016**, *51*, 395–411. [[CrossRef](#)]
7. Gao, X.F.; Lei, J. Biophysics: Water-repellent legs of water striders. *Nature* **2004**, *432*, 36. [[CrossRef](#)]
8. Sun, T.L.; Feng, L.; Gao, X.F.; Jiang, L. Bioinspired surfaces with special wettability. *Acc. Chem. Res.* **2005**, *38*, 644–652. [[CrossRef](#)]
9. Neinhuis, C.; Barthlott, W. Characterization and distribution of water-repellent, self-cleaning plant surfaces. *Ann. Bot.* **1997**, *79*, 667–677. [[CrossRef](#)]
10. Wang, S.L.; Liu, C.Y.; Liu, G.C.; Zhang, M.; Li, J.; Wang, C.Y. Fabrication of superhydrophobic wood surface by a sol-gel process. *Appl. Surf. Sci.* **2011**, *258*, 806–810. [[CrossRef](#)]
11. Shah, S.M.; Zulfiqar, U.; Hussain, S.Z.; Ahmad, I.; Rehman, H.U.; Hussain, I.; Subhani, T. A durable superhydrophobic coating for the protection of wood materials. *Mater. Lett.* **2017**, *203*, 17–20. [[CrossRef](#)]
12. Kang, S.M.; You, I.; Cho, W.K.; Shon, H.K.; Lee, T.G.; Choi, I.S.; Karp, J.M.; Lee, H. One-step modification of superhydrophobic surfaces by a mussel-inspired polymer coating. *Angew. Chem. Int. Ed. Engl.* **2010**, *49*, 9401–9404. [[CrossRef](#)] [[PubMed](#)]
13. Wu, Y.Q.; Jia, S.S.; Qing, Y.; Luo, S. A versatile and efficient method to fabricate durable superhydrophobic surfaces on wood, lignocellulosic fiber, glass, and metal substrates. *J. Mater. Chem. A* **2016**, *4*, 14111–14121. [[CrossRef](#)]
14. Yang, Y.S.; Shen, H.J.; Qin, L.; Qiu, J. Biomimetic fabrication of lotus-leaf-like self-cleaning superhydrophobic wood surface with micro/nano-biomimetic structures using morph-genetic method. *J. For. Eng.* **2020**, *5*, 66–71.
15. Che, Z.N.; Liu, G.C.; Guo, C.G.; Li, H.; Chen, R.J. Super-hydrophobic modification investigation for PTFE hollow fiber membrane surface based on the synergy of perfluorinated silane and alkylated SiO₂. *China Plast. Ind.* **2020**, *48*, 19–23.
16. Ntelia, E.; Karapanagiotis, I. Superhydrophobic paraloid B72. *Prog. Org. Coat.* **2020**, *139*, 105224. [[CrossRef](#)]
17. Bohinc, K.; Dražič, G.; Fink, R.; Oder, M.; Jevšnik, M.; Nipič, D.; Godič-Torkar, K.; Raspor, P. Available surface dictates microbial adhesion capacity. *Int. J. Adhes. Adhes.* **2014**, *50*, 265–272. [[CrossRef](#)]
18. Yue, D.; Feng, Q.F.; Huang, X.T.; Zhang, X.X.; Chen, H.X. In situ fabrication of a superhydrophobic ORMOSIL coating on wood by an ammonia-HMDS vapor treatment. *Coatings* **2019**, *9*, 556. [[CrossRef](#)]
19. Ghazali, N.; Basirun, W.J.; Nor, A.M.; Johan, M.R. Super-amphiphobic coating system incorporating functionalized nano-Al₂O₃ in polyvinylidene fluoride (PVDF) with enhanced corrosion resistance. *Coatings* **2020**, *10*, 387. [[CrossRef](#)]

20. Li, Z.N.; Deng, Z.W. Progress in research and application of mussel-inspired adhesive dopamine. *Polym. Mater. Sci. Eng.* **2015**, *31*, 185–190.
21. Guo, Q.; Chen, J.S.; Wang, J.L.; Zeng, H.G.; Yu, J. Recent progress in synthesis and application of mussel-inspired adhesives. *Nanoscale* **2020**, *12*, 1307–1324. [[CrossRef](#)] [[PubMed](#)]
22. Wang, Z.X.; Yang, H.C.; He, F.; Peng, S.Q.; Li, Y.X.; Shao, L.; Darling, S.B. Mussel-inspired surface engineering for water-remediation materials. *Matter* **2019**, *1*, 115–155. [[CrossRef](#)]
23. Jiang, L.; Jin, G.C.; Kang, J.Y.; Yu, L.M.; Yoon, W.; Lim, M.J.; Par, K.I.; Lee, M.; Jin, D.C. Surface characteristics of mussel-inspired polydopamine coating on titanium substrates. *J. Wuhan Univ. Technol.* **2014**, *29*, 197–200. [[CrossRef](#)]
24. Sun, Y.J.; Zhang, L.J.; Zhao, Y.Q.; Tang, Z.H.; Duan, S. Functionalized dental implants with antibacterial surface based on surface initiated polymerization. *Surf. Technol.* **2019**, *48*, 237–240.
25. Zhang, C.; Gong, L.; Xiang, L.; Du, Y.; Hu, W.J.H.; Zeng, H.B.; Xu, Z.K. Deposition and adhesion of polydopamine on the surfaces of varying wettability. *ACS Appl. Mater. Interf.* **2017**, *9*, 30943–30950. [[CrossRef](#)]
26. Ponzio, F.; Barthes, J.; Bour, J.; Michel, M.; Bertani, P.; Hemmerlé, J.; d’Ischia, M.; Vincent, B. Oxidant control of polydopamine surface chemistry in acids: A mechanism-based entry to superhydrophilic-superoleophobic coatings. *Chem. Mater.* **2016**, *28*, 4697–4705. [[CrossRef](#)]
27. Xue, C.H.; Deng, L.Y.; Jia, S.T.; Wei, P.B. Fabrication of superhydrophobic aromatic cotton fabrics. *RSC Adv.* **2016**, *6*, 107364–107369. [[CrossRef](#)]
28. Wang, K.L.; Dong, Y.M.; Yan, Y.T.; Zhang, S.F. Mussel-inspired chemistry for preparation of superhydrophobic surfaces on porous substrates. *RSC Adv.* **2017**, *7*, 29149–29158. [[CrossRef](#)]
29. Lee, H.; Dellatore, S.M.; Miller, W.M.; Miller, W.M.; Messersmith, P.B. Mussel-inspired surface chemistry for multifunctional coatings. *Science* **2007**, *318*, 426–430. [[CrossRef](#)]
30. Tan, G.X.; Ouyang, K.Y.; Zhou, L.; Liu, Y.; Fan, J.D.; Li, W.P.; Zhang, L.; Ning, C.Y. The mechanism of pH-induced polydopamine films surface protonation and cell adhesion behavior. *Sci. Sin.* **2016**, *46*, 373–381.
31. Della Vecchia, N.F.; Luchini, A.; Napolitano, A.; D’Errico, G.; Vitiello, G.; Szekely, N.; d’Ischia, M.; Paduano, L. Tris buffer modulates polydopamine growth, aggregation, and paramagnetic properties. *Langmuir* **2014**, *30*, 9811–9818. [[CrossRef](#)] [[PubMed](#)]
32. Wei, H.L.; Ren, J.; Han, B.; Xu, L.; Han, L.L.; Jia, L.Y. Stability of polydopamine and poly(DOPA) melanin-like films on the surface of polymer membranes under strongly acidic and alkaline conditions. *Coll. Surf. B Biointerf.* **2013**, *110*, 22–28. [[CrossRef](#)] [[PubMed](#)]
33. Kumar, A.; Richter, J.; Tywoniak, J.; Hajek, P.; Adamopoulos, S.; Šegedin, U.; Petrič, M. Surface modification of Norway spruce wood by octadecyltrichlorosilane (OTS) nanosol by dipping and water vapour diffusion properties of the OTS-modified wood. *Holzforschung* **2018**, *72*, 45–56. [[CrossRef](#)]
34. Wang, Z.L.; Ou, J.F.; Wang, Y.; Xue, M.S.; Wang, F.J.; Pan, B.; Li, C.Q.; Li, W. Anti-bacterial superhydrophobic silver on diverse substrates based on the mussel-inspired polydopamine. *Surf. Coat. Technol.* **2015**, *280*, 378–383. [[CrossRef](#)]
35. Qin, Z.Y.; Zhang, Q.; Gao, Q.; Li, J.Z. Wettability of sanded and aged fast-growing poplar wood surfaces: II. dynamic wetting models. *Bioresources* **2014**, *9*, 7176–7188. [[CrossRef](#)]
36. Wang, J.L.; Li, B.C.; Li, Z.J.; Ren, K.F.; Jin, L.J.; Zhang, S.M.; Chang, H.; Sun, Y.X.; Ji, J. Electropolymerization of dopamine for surface modification of complex-shaped cardiovascular stents. *Biomaterials* **2014**, *35*, 7679–7689. [[CrossRef](#)]
37. Su, X.; Peng, Y.F. Theoretical progress of superhydrophobic surfaces and its influencing factors. *J. Funct. Mater.* **2016**, *47*, 1–9.
38. Lou, S. Fabrication and Test of Superhydrophobic Surfaces Modified by Silicon Materials. Master’s Thesis, Tianjin University, Tianjin, China, May 2018.

